Vibration Mitigation of Nonlinear Vibrating Structures using Nonlinear Energy Sinks

R. Viguié[(1)], M. Peeters[(1)], G. Kerschen[(1)], J.C. Golinval[(1)]

(1) Structural Dynamics Research Group
Aerospace & Mechanical Engineering Department
University of Liège, Liège, Belgium
E-mail: r.viguie,m.peeters,g.kerschen,jc.golinval@ulg.ac.be

ABSTRACT

The tuned mass damper (TMD) is a simple and efficient device, but it is only effective when it is precisely tuned to the frequency of a vibration mode. Because nonlinear vibrating structures have resonant frequencies that vary with the amount of total energy in the system, the efficiency of a TMD is questionable in this case. In the present study, the performance of an essentially nonlinear attachment, termed a nonlinear energy sink (NES), is assessed. It is shown that, unlike the TMD, an NES has no preferential resonant frequency, which makes it a good candidate for vibration mitigation of nonlinear vibrating structures.

1 INTRODUCTION

The study dedicated to the dynamics of a linear oscillator (LO) coupled to a nonlinear energy sink (NES) has already been extensively treated in the literature [1−10]. The results emanating from these studies have put forward two remarkable properties that characterize the NES : (i) it has no preferential resonant frequency, which enables it to engage in resonance with any mode of the system, irrespective of the frequency range, (ii) Targeted Energy Transfer (TET) from a primary structure to an attached NES can be achieved through either single resonance captures, or resonance capture cascades.

However, even if from a theoretical viewpoint, the new dynamics created is of high interest, the question about the utility of using an NES to damp out vibrations of a LO, can be raised. Indeed, a LO possesses only one invariant resonant frequency and linear theories developed by Frahm [11] and Den Hartog [12] have clearly defined how to design an optimal linear dynamical vibration absorber (also called Tuned Mass Damper (TMD)) to damp out the vibrations submitted to such a primary structure. Moreover, the use of these design processes has shown that very good results can be reached whatever the criteria (performance or robustness) considered for the optimization scheme. According to these observations, an NES is certainly meaningful in the case of a MDOF primary structure or in the case of a SDOF structure submitted to mistuning.

Throughout this work, we consider a nonlinear SDOF primary system and in particular the Duffing oscillator. This system possesses a frequency-amplitude dependence that prevents us from using a TMD to damp out vibrations. Indeed, in this case the resonant frequency varies with the amplitude of excitation. The property of no preferential resonant frequency of the NES seems to make this device very well suited to damp vibrations on Duffing oscillators, whatever the amplitude of excitation. The resulting 2DOF system is depicted in Figure 1.

Even if the dynamics related to the introduction of an NES on a nonlinear primary structure has never been addressed from a general viewpoint, it has already been introduced on some nonlinear primary structures on which, self-sustained vibrations take place. As examples, one can note the LCOs that appear on an airplane wing [13] or on the drill-string system [14] submitted to

the flutter phenomena or a particular friction law, respectively. The results in both applications are very good and promising in perspective of the general study.

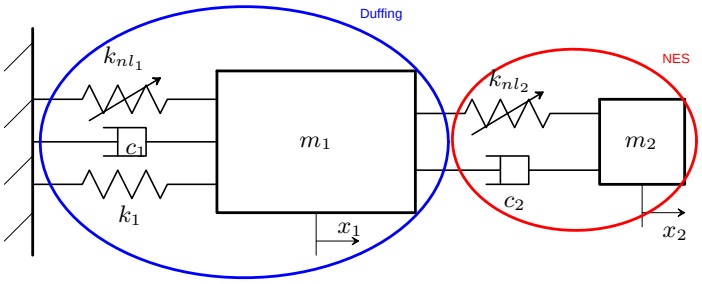

Figure 1: The 2DOF strongly nonlinear system.

In this study, the dynamics of the free conservative system will be addressed as it gives very good insight into the fundamental nonlinear mechanism occurring in the 2DOF system. The mechanisms of energy dissipation occurring in the impulsively forced and damped 2DOF system are assessed through the use of parametric studies as well as time and frequency analyzes. Finally, the harmonically forced dissipative configuration of the 2DOF system is investigated. In particular, the use of Nonlinear Frequency Response Functions (NL-FRFs) is shown to be very useful to characterize the nonlinear dynamics of the system, experimentally.

2 FREE RESPONSE OF THE CONSERVATIVE SYSTEM : FEP COMPUTATION

Before analyzing the nonlinear energy pumping phenomena that occurs in the damped system (Figure 1), it is necessary to first examine the structure of the periodic orbits of the underlying undamped system (with c_1 = c_2 = 0). Indeed, this seemingly simple system possesses a very complicated structure of periodic orbits, some of which are responsible for energy pumping phenomena in the impulsively forced and damped system. The corresponding equations of motion are given by :

$$\begin{cases} m_1\ddot{x}_1 + k_1x_1 + k_{nl_1}x_1^3 + k_{nl_2}(x_1 - x_2)^3 &= 0, \\ m_2\ddot{x}_2 + k_{nl_2}(x_2 - x_1)^3 &= 0. \end{cases} \tag{1}$$

with the following set of parameters :

Parameter	Units	Value	Parameter	Units	Value
m_1	$[kg]$	1	m_2	$[kg]$	0.05
k_{nl_1}	$[N/m^3]$	0.5	k_{nl_2}	$[N/m^3]$	1
k_1	$[N/m]$	1			

TABLE 1: Parameters values.

As mentioned in the introduction, nonlinear dynamical systems present a frequency-amplitude dependence. Therefore, the dynamics is highly influenced by the amplitude of the excitation imposed as well as by the order of magnitude of the nonlinear character of the system. Moreover, another key feature of nonlinear systems lies in the possibility to get several solutions, namely, periodic orbits, for a given level of energy injected in the system.

In order to get a good picture of the dynamics of the system, these two main properties of nonlinear systems have to be considered. A very interesting tool, called Frequency-Energy Plot (FEP) (introduced for the first time in [9]), gathers all this information on a single plot. In this section, only a basic description of the FEP concept is given and for further information, the interested reader may refer to [5, 9, 10, 15].

2.1 The Frequency-Energy Plot (FEP)

The FEP gathers all the periodic orbits of the considered system computed using analytical or numerical methods. The horizontal and vertical axis of this plot correspond to the amount of energy injected in the system and to the pulsation of the motion, respectively. The plot itself is composed of several branches, each of them being a collection of periodic solutions with the same characteristics. Without going into too many details, several key features of the FEP have to be described :

1. All the periodic orbits that characterize the system can be classified into two distinct families of solutions, the symmetric and the unsymmetric ones, denoted by S and U, respectively. The symmetric solutions are defined as periodic orbits that satisfy the condition **x**(t) = - **x**(t+$\frac{T}{2}$) with **x** corresponding to the state vector and T to the period of the motion, whereas periodic orbits that do not satisfy this condition are classified as unsymmetric solutions. Moreover, a periodic orbit belongs to a specific family of Nonlinear Normal Mode (NNM).
2. Two subscripts are added to the family category (S or U). They indicate the two main frequency contribution in the motion considered. More physically, in our 2DOF system (1), it describes how fast the DOFs are vibrating with respect to each other. Moreover, if we have S_{mn} or U_{mn}, it can be shown that m and n correspond to the primary system and the NES, respectively.

The FEP can be computed using analytical or numerical techniques. Both approaches have been addressed and the related results are displayed in the coming sections.

2.2 Analytical Computation Methods

To analytically compute the FEP, the Harmonic Balance method [16] and the Complexification Averaging Technique [17] are considered herein. Both methods are based on the assumption that the system motion can be approximated by means of a finite Fourier series. However, the harmonic balance method is limited to the study of the steady-state behavior whereas the complexification/averaging technique can also assess the transient dynamics of the motion. As the FEP determination only requires the analysis of the steady-state behavior, both methods can be applied. In this paper, only the main results are described (Figure 2) and the interested reader may refer to [18] for more details about the calculation process.

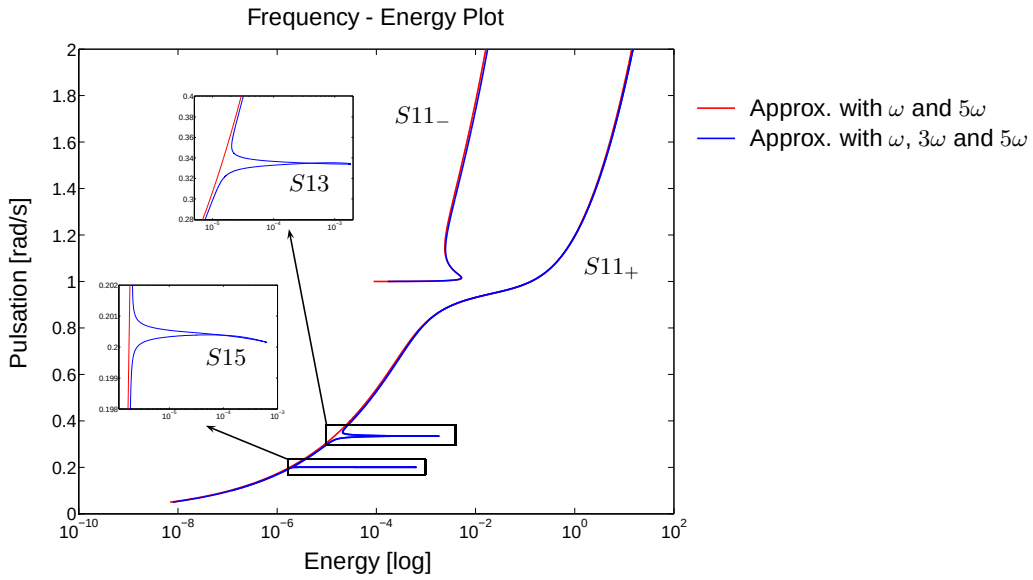

Figure 2: FEP computed using analytical methods.

The computation process as well as the result depicted in Figure 2 lead to some major comments :

1. Because analytical solutions are available in a limited number of cases, numerical methods are often used to solve the resulting system equations. The harmonic balance and complexification/averaging methods can therefore be viewed as

semi-analytical techniques.

2. The number of harmonics required in the approximation of the motion, to get a particular periodic orbit may vary according to their importance in the considered motion. As an example, Figure 2 shows that the third harmonic is required to get the S15 tongue (1:5 internal resonance).

3. Finally, seemingly to the methods based on series theories, the more components (namely, the harmonics) in the approximation the closer to the exact solution.

2.3 Numerical Computation Methods

The accuracy of the results obtained using analytical methods depends on the quality of the approximation of motion. This limitation can be avoided by considering specific numerical methods for the NNM computation such as the shooting or continuation methods. Indeed, these methods are dealing with the state space equations of the system that correspond to the exact formulation of the problem. The aim of this paper does not consist in going into the details of these methods and for further information on the subject, the interested reader may refer to [18−20]. However, it is worth being mentioned that the FEP computation has been achieved using the well known pseudo-arclength continuation method, based on a predictor and corrector step.

The continuation method is carried out in the continuation space (i.e. the ICs that lead to periodic motions) whereas the computation of the FEP is related to the frequency-energy space. Therefore, a post-processing of the continuation results is required to compute the energy. Knowing that the phase condition (in the continuation process) is such that velocities are zero for $t = 0$, this means that amplitudes at both DOF are maximum. Moreover, as the system is conservative, the total energy in the system consists in the potential energy stored in the stiffnesses at $t = 0$:

$$\text{Energy} = \frac{(x_1(0))^2}{2} + 0.5\,\frac{(x_1(0))^4}{4} + \frac{(x_1(0) - x_2(0))^4}{4} \tag{2}$$

and the Frequency-Energy Plot (FEP) corresponding to this system is depicted in Figure 3. It is composed of two backbones ($S11_+$ and $S11_-$) corresponding to in phase and out-of-phase $1:1$ fundamental resonance motion, respectively. Moreover, theoretically, an infinite countable number of tongues, corresponding to internal resonances, are emanating from these backbones. Herein, only some subharmonic ($S13$,$S15$,$S17$,$S19$) and superharmonic ($U21$,$S31$) tongues are illustrated.

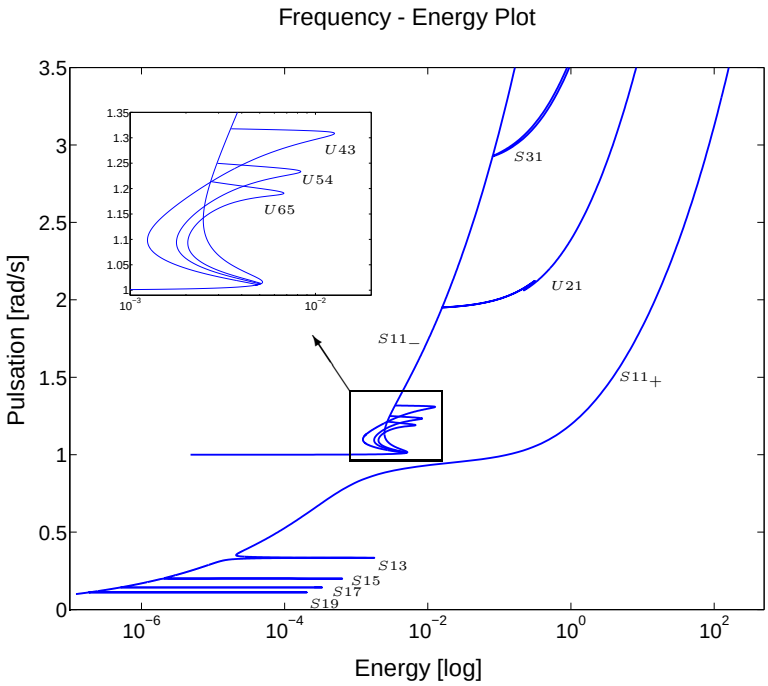

Figure 3: FEP of the 2DOF strongly nonlinear system.

2.4 Characterization of the FEP

Some of the branches can be analyzed to give a basic idea on how the NNMs evolve along a backbone or a tongue. To this end, the representation of the motion at both DOFs is illustrated in the configuration space, over one period (insets in the Figures). The vertical and horizontal axis correspond to the motion at the linear and nonlinear oscillators respectively. Moreover, the scale at both axis is the same so that it can be directly deduced where the motion is localized.

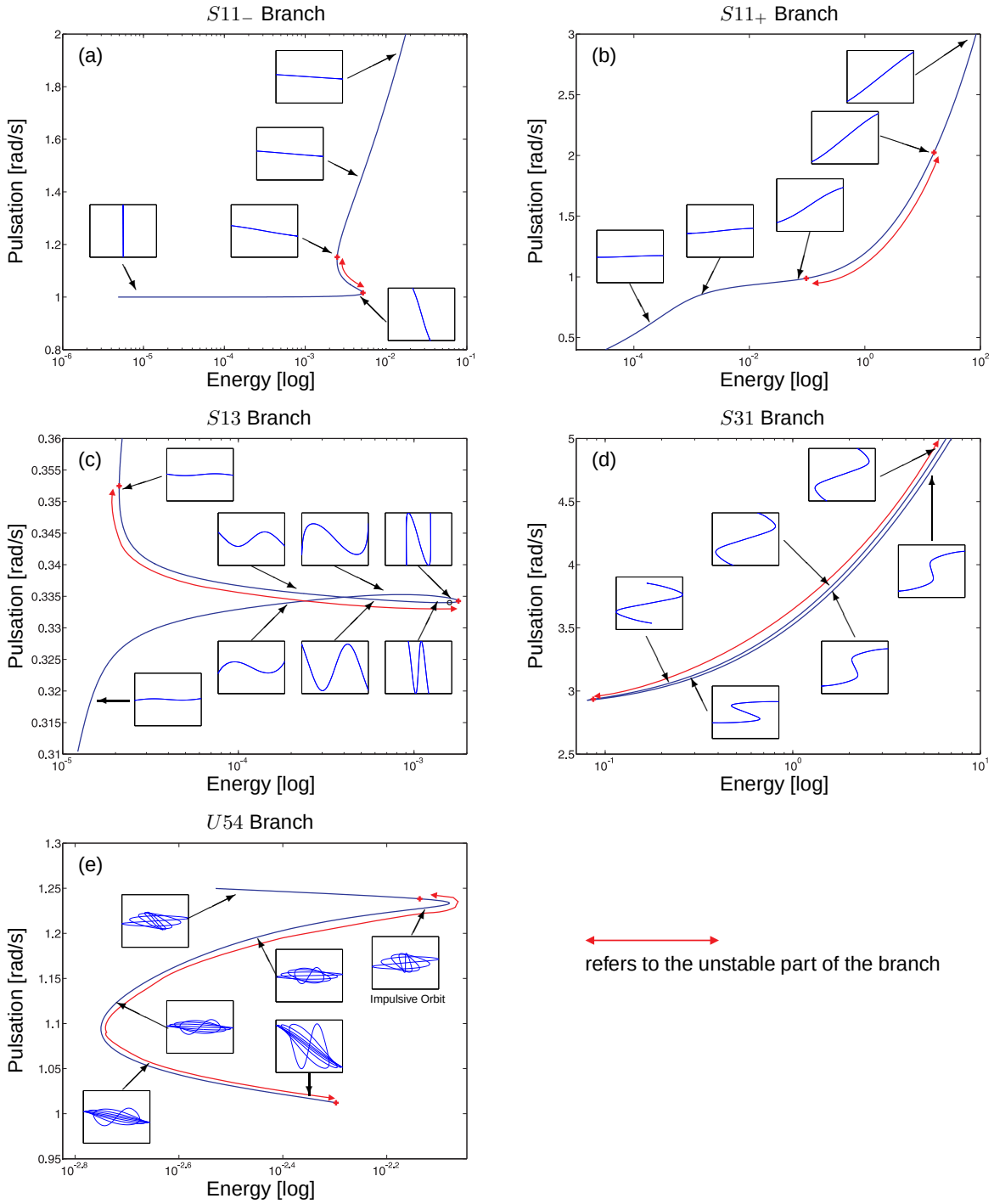

Figure 4: Families of NNM motions.

Figures 4 (a to e) give a better understanding on the different type of NNM motions that take place in different frequency-energy domains and some major comments can be formulated :

- On $S11_-$ (Figure 4 a), stable solutions become localized to the linear or nonlinear oscillator as $\omega \rightarrow 1^+$ or $\omega >>>$, respectively.
- On $S11_+$ (Figure 4 b), at low energy level, the motion is localized in the nonlinear oscillator until we reach an unstable region whereas at higher energy level, the motion tends toward infinity in a stable fashion.
- For $S13$ and $S31$ branch , (Figure 4 c and d) the third harmonic plays a major part in the nonlinear oscillator or in the linear one, respectively. Moreover, unlike the $S13$ tongue, branch $S31$ is characterized by a asymptotical behavior for an energy level that tends toward infinity.
- Figure 4(e) represents a family of unsymmetrical NNM motion. In this case, the shape in the configuration phase consists in a closed loop. Moreover, the impulsive orbit (defined in the next paragraph) is characterized, as expected, by a vertical slope at the origin of the configuration plane.

Locus of Impulsive Orbits

Some periodic orbits of the families of NNMs are of particular importance in the experimental study of the energy transfer occuring in nonlinear systems. These orbits satisfy the initial condition : $x_1 = x_2 = \dot{x}_2 = 0$ and $\dot{x}_1 \neq 0$ that correspond to the state of the undamped system (being initially at rest) after the application of an impulse on the first DOF. It has been highlighted in [21] that *the impulsive excitation of one of the stable impulsive orbits is one of the triggering mechanisms initiating (direct) passive energy pumping*. Finally, it can be mentioned that in the configuration space, these orbits always pass through the origin with a vertical slope (an example is given in Figure 4(e)). Figure 5 represents the position of some impulsive orbits (red circles) as well as an estimate of the locus of all the existing impulsive orbits (black dotted line).

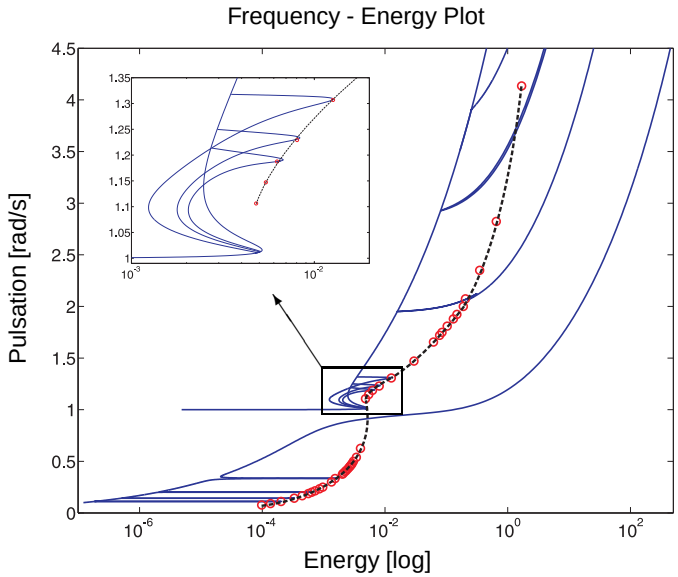

Figure 5: Locus of special orbits.

3 MECHANISMS OF ENERGY DISSIPATION IN THE FREE DISSIPATIVE SYSTEM

This section aims to study the mechanisms of energy dissipation occurring in the system depicted in Figure 1 and submitted to impulsive excitation condition at the first DOF. To this end, 3D plots of energy dissipated by the NES versus the nonlinear stiffness of the primary system (k_{nl_1}) and the impulse ($\dot{x}_1$) are computed. These plots can be seen as pictures of the performance and robustness of the NES with respect to mistuning in the primary system or varying excitation conditions. The energy dissipated

by the absorber can be worked out as follows :

$$E_{dissip}(t) = \frac{E^{abs}_{dissip}(t)}{E_{injected}(t)} \equiv \frac{c_2 \int_0^t (\dot{x}_1 - \dot{x}_2)^2 d\tau}{\int_0^{t_{max}} p(\tau)\dot{y}(\tau) d\tau} = \frac{c_2 \int_0^t (\dot{x}_1 - \dot{x}_2)^2 d\tau}{\frac{1}{2} m_1 \dot{x}_1^2(0)} \tag{3}$$

The corresponding 3D plot is depicted in Figure 6(a). It can be noticed the presence of some ridges of high energy dissipation levels. To get a better insight into the borders of these ridges, the projection (of the energy dissipated) in the plane (k_{nl_1},$\dot{x}_1$) is carried out and five distinct regions are identified (Figure 6(b)). Moreover, if some points in this plane were considered and the corresponding FEP computed, it could be highlighted that only the positions of the superharmonic tongues are fluctuating a lot whereas the subharmonic tongues and the backbone $S11\_$ keep similar. This feature seems to explain that the regions of high energy dissipation are characterized by superharmonic motions. For further details on the subject, the interested reader may refer to [18]. In this paper, the focus is set on the time and frequency analyzes of the motions taking place in the aforementioned regions.

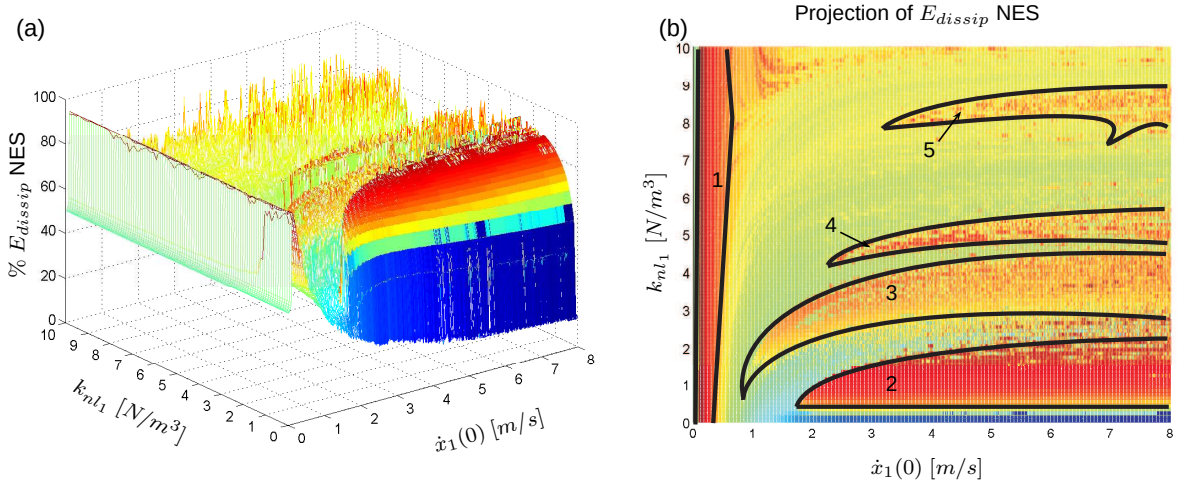

Figure 6: (a)3D plot of the energy dissipated by the NES / (b) Projection of the 3D plot.

3.1 Analysis of Numerical Simulations

This paragraph is concerned with the time and frequency analyzes of the motions occurring in the different areas identified in Figure 6(a).

3.1.1 ANALYSIS OF THE FIRST AREA

This area of high interest corresponds to the region where the best level of energy dissipated by the NES is observed ($\pm 95\%$). To this end, the analyzes are performed for a particular system configuration ($k_{nl_1} = 9N/m^3$ and $\dot{x}_1(0) = 0.13m/s$). However, it can be shown that the behavior is the same for the remaining configurations of the area. The related results are depicted in Figure 7.

The time evolution of the motion (Figure (a)) shows a relatively fast damping process. Indeed, after 300 seconds both amplitudes are drastically reduced. Moreover, the total amount of energy dissipated by the absorber (Figure (d)) is a very good 93% of the energy injected in the system. The reason for such a good energy dissipation lies in the excitation of a particular special orbit that belongs to families of unsymmetrical NNMs such as $U_{k,k+1}$ with $k = 1, 2, ...$ as explained is [5, 9, 10, 15, 21]. Indeed, these orbits create the nonlinear beating phenomenon that is the triggering mechanism for the occurrence of targeted energy transfer from the primary structure to the NES. In the present application, the impulsive orbit belongs to branch $U54$ (Figure (f)) and the nonlinear beating phenomenon is clearly highlighted in Figure c where strong energy exchanges between both DOFs take place during the first 50 seconds. Then the NES engages in a $1:1$ fundamental resonance (between 75 and 160 seconds) with the

primary system (on $S11_+$ in Figure (f)). During this phase, the amplitude of the NES is larger than the one of the primary system; this indicates that energy pumping takes place from the primary mass to the NES. As energy decreases, the motion transits for very short periods from $S11_+$ to $S13$, $S15$,... (Figures e-f).

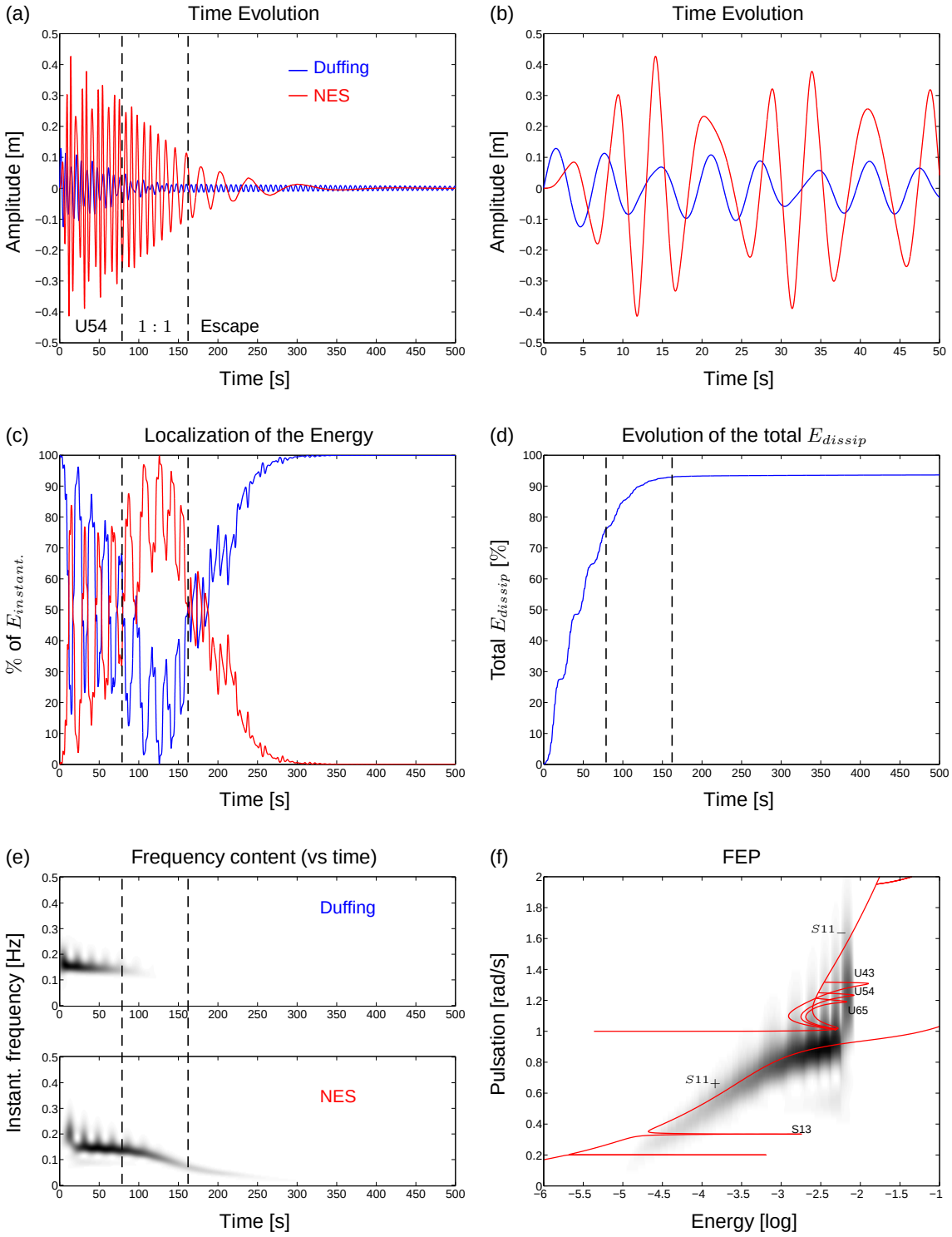

Figure 7: Dynamical analysis of a given configuration for the 2-DOF system corresponding to the first area (Figure 6(a)).

3.1.2 ANALYSIS OF THE OTHER AREAS

Note that in [18] a complete analysis has been carried out for all the ridges. Herein, as all these analyzes are very similar, only the final results are put forward. Because the characterization of ridges 4 and 5 is very difficult due to their high sensitivity to small pertubations, they are not analyzed into details. However, it can be proved that for ridges 2 and 3, $3:1$ and $2:1$ superharmonic motions ($S31$ and $U21$ respectively) are taking place during the beginning of the motion. Then, both are followed by $1:1$ fundamental resonance capture ($S11_+$). Figures 8 (a) and (b) clearly highlight this feature using the superposition of the wavelet transform results and the FEP of the considered system.

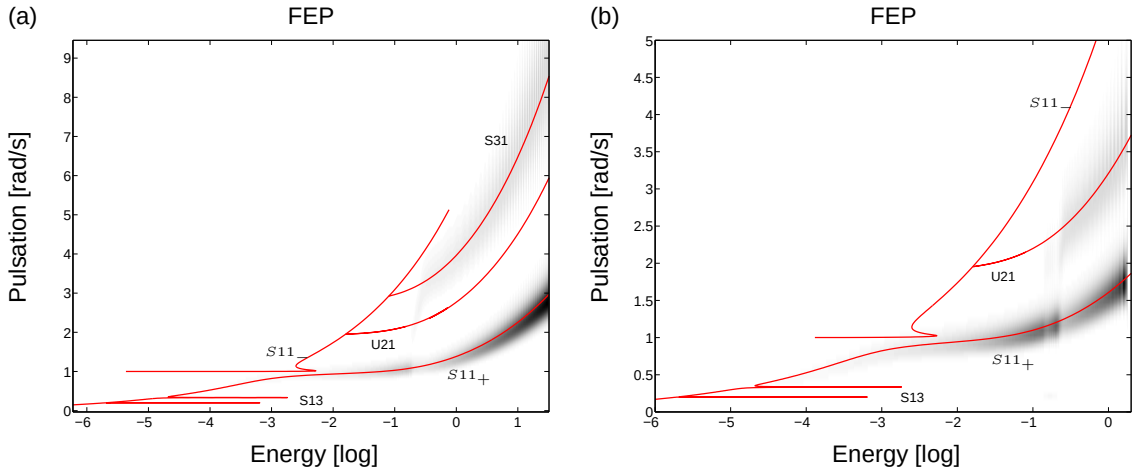

Figure 8: [(a)/(b)] frequency analyzes for the second and third area (Figure 6), respectively.

These results put forward the importance of the superharmonic motions in the mechanisms of energy dissipation whereas the subharmonic motions are not so involved. This feature consists in a major difference with the mechanisms of energy dissipation taking place in a system composed of a LO coupled to an NES (in [9]) where subharmonic motions frequently occur.

3.2 Effects created by the Variation of the NES Components

The previous section has shown the presence of regions with high energy dissipation levels. It is worth being known how these regions evolve with changing values of the NES components. To this end, 3D plots of energy dissipation are computed with the initial set of parameters (Table 2) and only one varying NES parameter.

3.2.1 INFLUENCE OF THE NONLINEAR STIFFNESS K_{NL_2}

The projections illustrated in Figure 9 highlight that a lower nonlinear stiffness value leads to the spreading of the first region (NL beating) over the expertise plane whereas an increase leads to the extension of the second region ($S31$ motion) and the narrowing of the first area. It can be concluded that an increase *(decrease)* of the nonlinear character of the NES induces the presence of nonlinear effects at lower *(upper)* excitation levels (consequently, a transfer of the areas toward lower *(upper)* excitation levels). It can be noted that this observation may be confirmed by the study of the localization of the related FEPs. For further details, the interested reader may refer to [18].

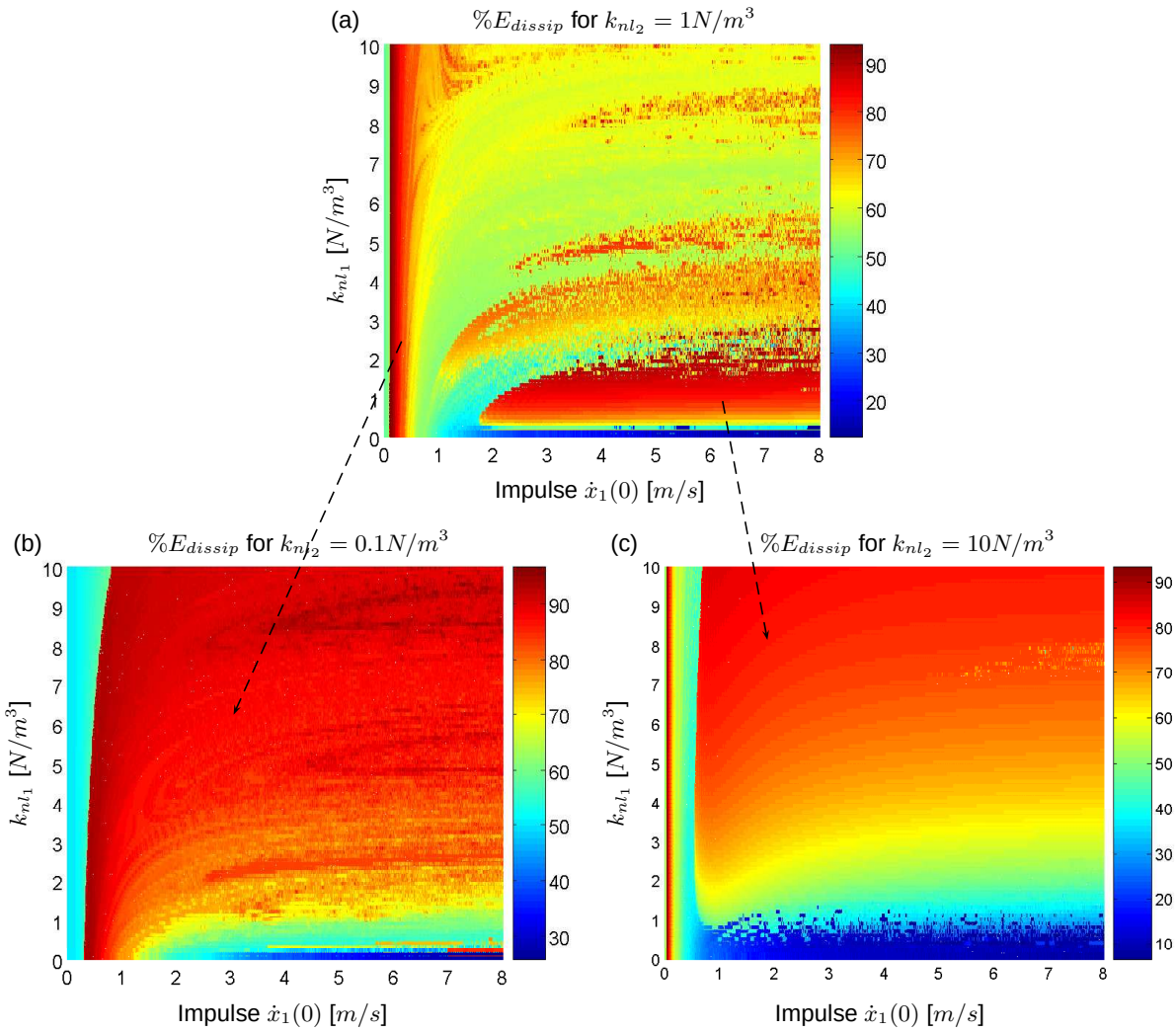

Figure 9: Influence of a varying value of the NES nonlinear stiffness on the energy dissipated in the absorber.

3.2.2 INFLUENCE OF THE DAMPING COEFFICIENT C_2

The projections illustrated in Figure 10 highlight that taking into account a higher value of damping create the same dynamical phenomena as for the initial system but for higher excitation levels. This can be understood as the damping kills the nonlinear effects that will only appear later for stronger excitations. Moreover, in addition to this statement, it can be noted a smoothening of the 3D surface of energy dissipation. It can be concluded that an increase *(decrease)* of the damping coefficient induces the transfer of the areas toward higher *(lower)* excitation levels.

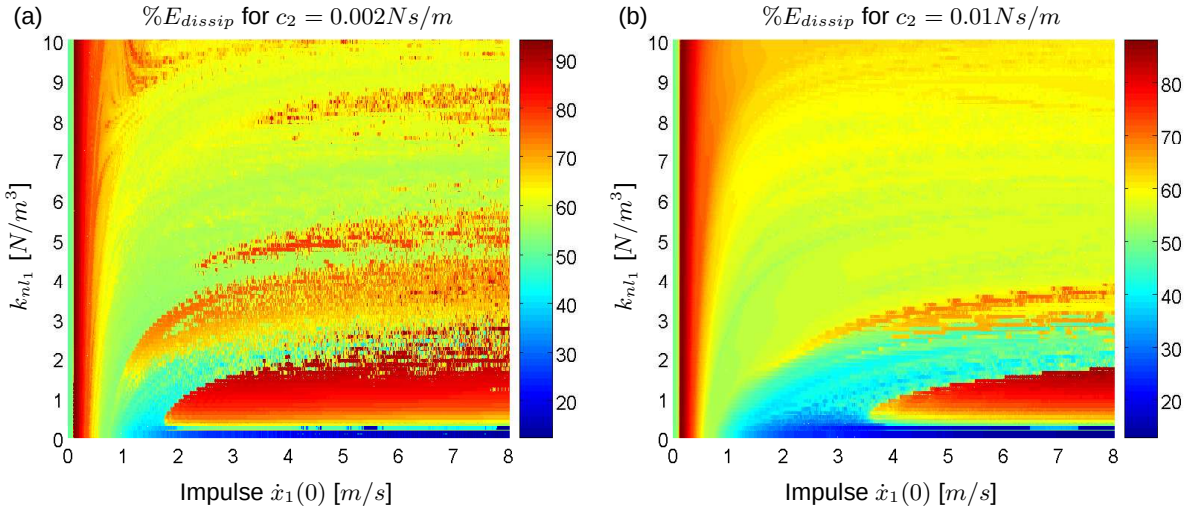

Figure 10: Influence of a varying value of the NES damping coefficient on the energy dissipated in the absorber.

4 TOWARD AN EXPERIMENTAL COMPUTATION OF THE FEP

In section 2, it has been shown how to compute the FEP using analytical or numerical approaches. However, it would be relevant to establish whether it is possible to retrieve it experimentally. To this end, the system under the scope is depicted in Figure 1 with a harmonic forcing applied on the first DOF and assuming a low damping level. The corresponding equations of motion are established in expressions 4 and the set of parameters considered in the study is referred in Table 2.

$$\begin{cases} m_1\ddot{x}_1 + c_1\dot{x}_1 + c_2(\dot{x}_1 - \dot{x}_2) + k_1x_1 + k_{nl_1}x_1^3 + k_{nl_2}(x_1 - x_2)^3 &= F\cos\omega t, \\ m_2\ddot{x}_2 + c_2\dot{x}_2 + k_{nl_2}(x_2 - x_1)^3 &= 0. \end{cases} \tag{4}$$

Parameter	Units	Value	Parameter	Units	Value
m_1	$[kg]$	1	m_2	$[kg]$	0.05
k_{nl_1}	$[N/m^3]$	0.5	k_{nl_2}	$[N/m^3]$	1
c_1	$[Ns/m]$	0.002	c_2	$[Ns/m]$	0.002
k_1	$[N/m]$	1			

TABLE 2: Parameters numerical value.

The objective lies in the determination of the nonlinear frequency response functions (NL-FRFs) of the system over a particular frequency range for a given external force level. The idea consists in showing the existing link between the branches of the FEP computed for the free conservative system and the peaks of the NL-FRFs of the nonconservative periodically forced system. Indeed, in this case, it will be proved that, first, the resonance occurs in the neighborhood of the corresponding NNM and second, the FEP can be experimentally retrieved. To this end, the continuation method developed for the free response case is adapted to the forced response case as the phase is not trivial anymore (for further details cf [18, 22–24]).

4.1 NL-FRF Computation

As the forced continuation process takes place in the continuation space $(\mathbf{x_{0p}}, T)$, a post-processing step (time integration over one period) of the results is required to extract all the couples $(\omega, |x_1(t)|_{max})$ and $(\omega, |x_2(t)|_{max})$ that compose the NL-FRFs at the first and second DOF, respectively. The frequency-energy dependence property is highlighted by holding on a series of NL-FRFs corresponding to different external force levels F (Figure 11 depicts the NL-FRFs at the first DOF). For further details about the computation as well as a complete characterization of this kind of plot, the interested reader may refer to [18].

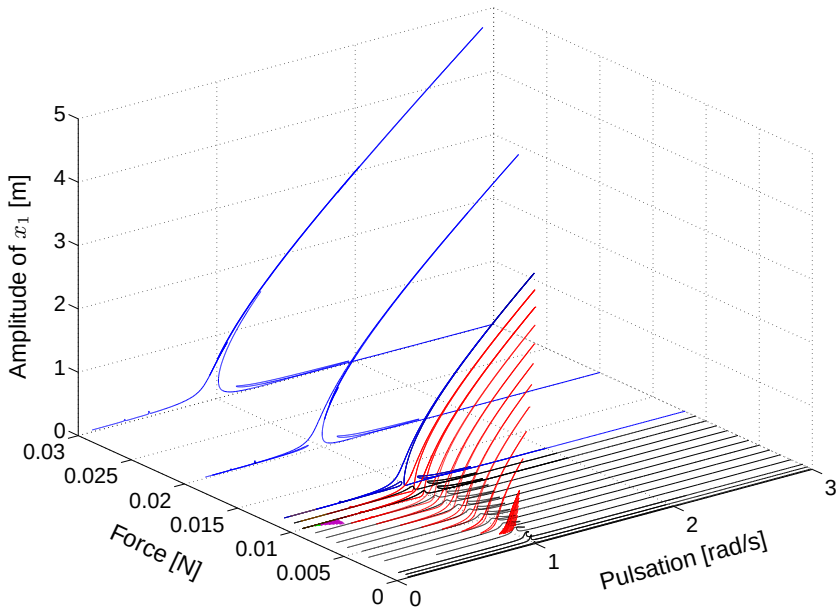

Figure 11: NL-FRFs at the first DOF.

4.2 FEP Computation using the NL-FRFs

The path-following technique applied to the free conservative system is characterized by a particular phase condition that imposes the initial velocities at both oscillators to be zero. Consequently, the initial displacements computed are maximum. Moreover, in the present chapter, several NL-FRFs have been worked out for given force (energy) levels. Each one of these NL-FRFs possesses several peaks corresponding to relative maximum displacements at one oscillator. Therefore, for a given oscillator, it is meaningful to compare, on one hand, the continuation branch of its displacements in the free conservative case and on the other hand, the locus formed by all the maximum points (the peaks) of the NL-FRFs in the forced dissipative case. In this chapter, only the $1:1$ fundamental resonance ($S11_-$ and $S11_+$) is studied. The pulsation corresponding to the peak of the NL-FRFs is easily determined whereas the related energy contained in the system (potential and kinetic) has to be worked out using the following relation :

$$\text{Energy(t)} = k_1 \frac{x_1^2(t)}{2} + k_{nl_1} \frac{x_1^4(t)}{4} + k_{nl_2} \frac{(x_1(t) - x_2(t))^4}{4} + m_1 \frac{\dot{x}_1^2(t)}{2} + m_2 \frac{\dot{x}_2^2(t)}{2} \tag{5}$$

Then, considering a given force level F, the link between the related NL-FRFs and the FEP can be established (Figure 12).

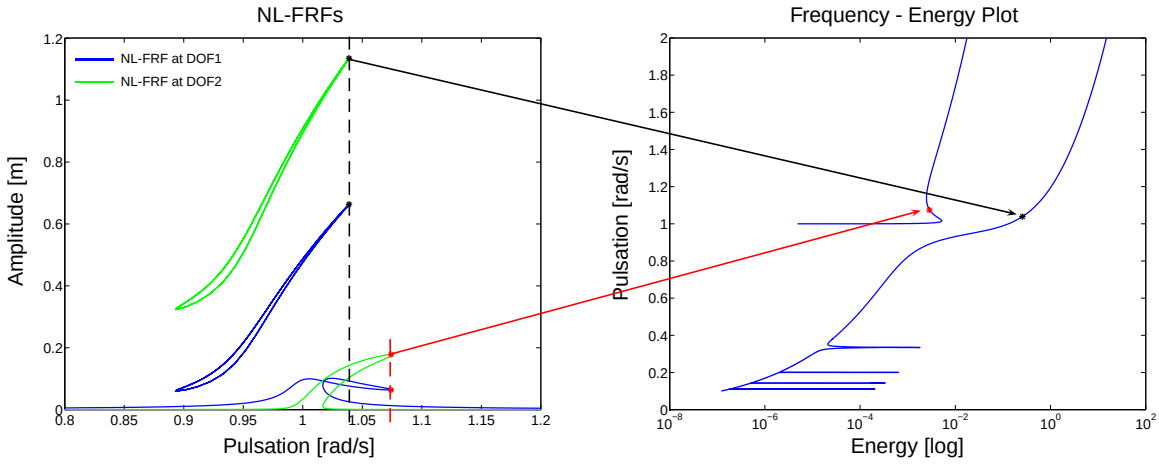

Figure 12: Link between the NL-FRFs and the FEP for a given force level F.

Now, extending this process to the whole range of NL-FRFs computed in Figure 11, both backbones ($S11_-$ and $S11_+$) can be retrieved (Figure 13).

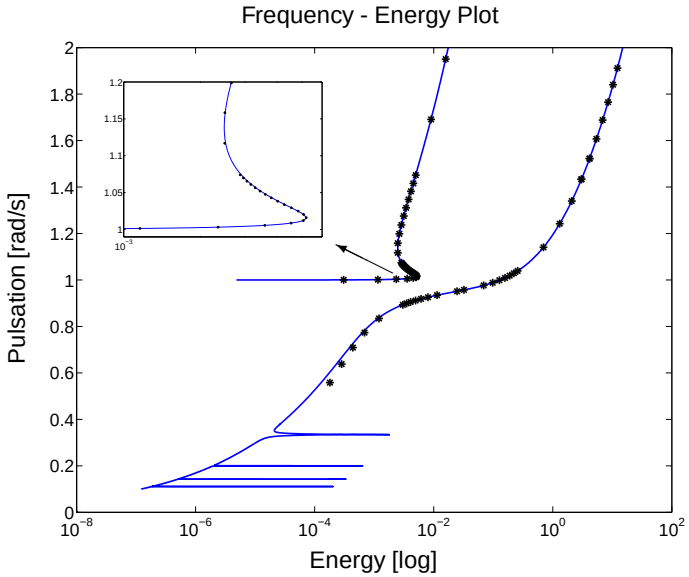

Figure 13: FEP experimentally retrieved.

Finally, it can be concluded that the FEP numerically computed for the free conservative system can also be experimentally computed. This also confirms that, seemingly to the linear case, the resonance occurs in the neighborhood of the related NNM.

5 CONCLUSION

The objective of this work was to study the dynamics created by the association of an NES to a nonlinear primary structure. To this end, the complicated dynamics related to the strongly nonlinear conservative 2DOF system has been analyzed and compiled in a single plot, numerically computed and called the Frequency-Energy Plot (FEP). Then, the families of NNM motions constituting the tongues of the FEP and representing the fundamental and internal resonances, have been fully characterized. Indeed seemingly to linear systems, the resonance occurs in the neighborhood of the corresponding NNM. Once the FEP of the system had been determined, parametric studies put forward the presence of different areas of high energy dissipation. The mechanisms responsible for this good energy dissipation have been identified as (i) the nonlinear beating phenomena that triggers energy pumping, (ii - iii) the superharmonic motions S31 and U21. The results related to the last performed parametric studies have shown that provided the primary system is well defined (in terms of stiffness and excitation conditions) an NES can be designed to ensure a given level of energy dissipation. Finally, it has also been shown that the FEP can be experimentally retrieved.

The next objectives are mainly focused on three different subjects :

1. Parametric studies are interesting as they give reliable results, however, they require a high computational cost. Therefore, currently, the development of a better suited methodology based on analytical concepts is investigated. The first results are very promising and more efforts have to be dedicated to this research path.

2. So far, mechanical constraints are imposed to the NES only because of practical considerations. As an example, the mass of the NES is always supposed to be lower than 5% of the primary mass. As it is well known that higher masses create better dynamical behaviors, the purpose would be to suppress this structural constraint. An interesting alternative lies in the use of the duality property existing between the motion equations of a mechanical system and those of an electrical circuit, also called electromechanical transduction. This property has already been broadly studied for the realization of an electrical Tuned Mass Damper. The concept consists in dissipating mechanical energy with piezoelectric material shunted with passive electrical circuits $^{[25-29]}$. In practice, these electrical devices consist in small patches and the drawbacks linked to the practical realization of TMD have no more importance. Therefore, according to the aforementioned discussion,

it seems that the development of an electrical NES through the use of piezoelectric material shunted to passive electrical circuits is meaningful and of great interest. Finally, it is worth being mentioned that the use of electrical component may be a very helpful solution to create any kind of nonlinear stiffness law.

Acknowledgments

The authors R. Viguié and G. Kerschen would like to acknowledge the Belgian National Fund for Scientific Research (FRIA & FNRS fellowships) for its financial support.

REFERENCES

[1] **Gendelman, O. V.**, *Transition of energy to a nonlinear localized mode in a highly asymmetric system of two oscillators*, Nonlinear dynamics, Vol. 25, pp. 237–253, 2001.

[2] **Gendelman, O. V., Manevitch, L. I., Vakakis, A. F.** and **McCloskey, R.**, *Energy pumping in nonlinear mechanical oscillators: Part I - Dynamics of the underlying Hamiltonian systems*, Journal of Applied Machanics, Vol. 68, pp. 34–41, January 2001.

[3] **Vakakis, A. F.** and **Gendelman, O. V.**, *Energy pumping in nonlinear mechanical oscillators: Part II - Resonance capture*, Journal of Sound and Vibration, Vol. 68, pp. 42–48, January 2001.

[4] **Vakakis, A. F.**, *Inducing passive nonlinear energy sinks in vibrating systems*, Journal of Vibration and Acoustics, Vol. 123, pp. 324–332, 2001.

[5] **Kerschen, G., Vakakis, A. F., Lee, Y. S., McFarland, D. M., Kowtko, J. J.** and **Bergman, L. A.**, *Energy transfers in a system of two coupled oscillators with essential nonlinearity: 1:1 resonance manifold and transient bridging orbits*, Nonlinear Dynamics, Vol. 42, pp. 289–303, 2005.

[6] **McFarland, D. M., Bergman, L. A.** and **Vakakis, A. F.**, *Experimental study of nonlinear energy pumping occurring at a single fast frequency*, International Journal of Non-Linear Mechanics, Vol. 40, pp. 891–899, 2005.

[7] **Kerschen, G., McFarland, D. M., Kowtko, J. J., Lee, Y. S., Bergman, L. A.** and **Vakakis, A. F.**, *Experimental demonstration of transient resonance capture in a system of two coupled oscillators with essential stiffness nonlinearity*, Journal of Sound and Vibration, Vol. 299, No. 4-5, pp. 822–838, February 2007.

[8] **Gendelman, O. V., Gorlov, D. V., Manevitch, L. I.** and **Musienko, A. I.**, *Dynamics of coupled linear and essentially nonlinear oscillators with substantially different masses*, Journal of Sound an Vibration, Vol. 286, pp. 1–19, 2005.

[9] **Lee, Y. S., Kerschen, G., Vakakis, A. F., Panagopoulos, P. N., Bergman, L. A.** and **McFarland, D. M.**, *Complicated dynamics of a linear oscillator with a light, essentially nonlinear attachment*, Physica D, Vol. 204, pp. 41–69, 2005.

[10] **Kerschen, G., Lee, Y. S., Vakakis, A. F., McFarland, D. M.** and **Bergman, L. A.**, *Irreversible passive energy transfer in coupled oscillators with essential nonlinearity*, SIAM Journal of Applied Mathematics, Vol. 66, No. 2, pp. 648–679, January 2006.

[11] **Frahm, H.**, A Device for Damping Vibrations of Bodies, US Patent 989958, 1911.

[12] **Den Hartog, J. P.**, Mechanical Vibrations, Dover Books on Engineering, 4th edn., 1985.

[13] **Lee, Y. S., Vakakis, A. F., Bergman, L. A., McFarland, D. M.** and **Kerschen, G.**, *Suppression of Aeroelastic Instability by Means of Broadband Passive Targeted Energy Transfers, Part I : Theory*, AIAA Journal, Vol. 45, No. 3, pp. 693–711, March 2007.

[14] **Viguié, R., Kerschen, G., Golinval, J.-C., McFarland, D. M., Bergman, L. A.** and **van de Wouw, N.**, *Using passive nonlinear targeted energy transfer to stabilize drill-string system*, Mechanical Systems and Signal Processing (in press), 2007.

[15] **McFarland, D. M., Kerschen, G., Kowtko, J. J., Lee, Y. S., Bergman, L. A.** and **Vakakis, A. F.**, *Experimental investigation of targeted energy transfers in strongly and nonlinearly coupled oscillators*, Journal Acoustical Society of America, Vol. 118, No. 2, pp. 791–799, August 2005.

[16] **Nayfeh, A. H.** and **Mook, D. T.**, Nonlinear Oscillations, Wiley-Interscience, New-York, 1995.

[17] **Manevitch, L. I.**, *Complex representation of dynamics of coupled oscillators*, Mathematical Models of Nonlinear Excitations, Transfer Dynamics and Control in condensed Systems, Kluwer Academic/Plenum Publishers, pp. 269–300, 1999.

[18] **Viguié, R.**, Passive Virbation Mitigation in Mechanical Systems using Nonlinear Energy Sinks, Master's thesis, University of Liege, September 2007.

[19] **Seydel, R.**, Practical Bifurcation and Stbility Analysis From Equilibrium to Chaos., Springer-Verlag, 2nd edn., 1994.

[20] **Peeters, M., Viguié, R., Sérandour, G., Kerschen, G.** and **Golinval, J.-C.**, *Nonlinear Normal Modes, Part 2 : Practical Computation using Numerical Continuation Techniques*, MSSP (in review), 2007.

[21] **Kerschen, G., McFarland, D. M., Kowtko, J. J., Lee, Y. S., Bergman, L. A.** and **Vakakis, A. F.**, *Impulsive periodic and quasi-periodic orbits of coupled oscillators with essential stiffness nonlinearity*, Communication in Nonlinear Science and Numerical Simulation (in press).

[22] **Padmanabhan, C.** and **Singh, R.**, *Analysis of periodically excited non-linear systems by a parametric continuation technique*, Journal of Sound and Vibration, Vol. 184, No. 1, pp. 35–58(24), 1995.

[23] **Sundararajan, P.** and **Noah, S. T.**, *Dynamics of forced nonlinear systems using shooting/arc-length continuation method - Application to rotor systems*, Journal of Vibration and Acoustics, Vol. 119, No. 1, pp. 9–20(19), January 1997.

[24] **Sundararajan, P.** and **Noah, S. T.**, *An algorithm for response and stability of large order non-linear systems - Application to rotor systems*, Journal of Sound and Vibration, Vol. 214, No. 4, pp. 695–723(29), July 1998.

[25] **Hagood, N. W.** and **von Flotow, A.**, *Damping of structural vibrations with piezoelectric materials and passive electrical networks*, Journal of Sound and Vibration, Vol. 146, No. 2, pp. 243–268, April 1991.

[26] **Preumont, A.**, Vibration Control of Active Structures : An introduction, Kluwer Academic Publishers, 1997.

[27] **J. Ducarne, J., Thomas** and **Deü, J. F.**, *Optimisation de dispositifs passifs dŠatténuation de vibration par shunt piézoélectrique*, Colloque national en calcul de structure, Giens, 2007.

[28] **Fleming, A. J.**, Synthesis and implementation of sensor-less shunt controllers for piezoelectric and electromagnetic vibration control, Ph.D. thesis, School of Electrical Engineering and Computer Science, The University of Newcastle Callaghan, Australia, February 2004.

[29] **Livet, S., Berthillier, M., Collet, M.** and **Cote, J.**, *Numerical and experimental optimized shunted piezoelectric circuit for turbomachinery blades*, 12th IFToMM World Congress, Besançon, June 18-21 2007.